

Characterization of functional groups in estuarine dissolved organic matter by DNP-enhanced ^{15}N and ^{13}C solid-state NMR

Florian Venel^a, Hiroki Nagashima^{a,e}, Andrew G.M. Rankin^{a,f}, Christelle Anquetil^b, Vytautas Klimavicius^{c,g}, Torsten Gutmann^c, Gerd Buntkowsky^c, Sylvie Derenne^b, Olivier Lafon^{a,d*}, Arnaud Huguet^b and Frédérique Pourpoint^{a*}

*a. F. Venel, Dr. H. Nagashima, Dr. A. G. M. Rankin, Prof. O. Lafon, Dr. F. Pourpoint
Univ. Lille, CNRS, Centrale Lille, Univ. Artois, UMR 8181 – UCCS – Unité de Catalyse et Chimie du Solide, F-59000 Lille, France*

Email : olivier.lafon@univ-lille.fr, frederique.pourpoint@centralelille.fr

*b. C. Anquetil, Dr. S. Derenne, Dr. A. Huguet
Sorbonne Univ, UMR 7619 Metis, CNRS, EPHE, PSL, 4 Place Jussieu, F-75252 Paris 05, France.*

*c. Dr. V. Klimavicius, Dr. T. Gutmann, Prof. G. Buntkowsky
Institute of Physical Chemistry, Technical University Darmstadt, Alarich-Weiss-Straße 8, D-64287 Darmstadt, Germany*

*d. , Prof. O. Lafon,
Institut Universitaire de France, 1 rue Descartes, 75231 Paris, France.*

*e. , Dr. H. Nagashima
Interdisciplinary Research Center for Catalytic Chemistry, National Institute of Advanced Industrial Science and Technology (AIST), 1-1-1 Higashi, Tsukuba, Ibaraki 305-8565, Japan*

*f. Dr. A. G. M. Rankin
Sorbonne Univ., LCMCP UMR 7475, CNRS, CdF, 4 place Jussieu, F-75252 Paris 05, France*

*g. Dr. V. Klimavicius
Institute of Chemical Physics, Vilnius University, Sauletekio av. 3, LT-10257 Vilnius, Lithuania*

Electronic Supplementary Information (ESI) available: [conventional $^1\text{H} \rightarrow ^{13}\text{C}$ CPMAS NMR spectra].

Abstract:

Estuaries are key ecosystems with unique biodiversity and high economic importance. Along the estuaries, variations in environmental parameters, such as salinity and light penetration, can modify the characteristics of Dissolved Organic Matter (DOM). Nevertheless, there is still limited information about the atomic-level transformations of DOM in this ecosystem. Solid-state NMR spectroscopy provides unique insights into the nature of functional groups in DOM. A major limitation of this technique is its lack of sensitivity, which results in experimental time of tens of hours for the acquisition of ^{13}C NMR spectra and generally precludes the observation of ^{15}N nuclei for DOM. We show here how the sensitivity of solid-state NMR experiments on DOM of Seine estuary can be enhanced using dynamic nuclear polarization under magic-angle spinning. This technique allows the acquisition of ^{13}C NMR spectra of these samples in a few minutes, instead of a few hours for conventional solid-state NMR. Both conventional and DNP-enhanced ^{13}C NMR spectra indicate that the ^{13}C local environments in DOM are not strongly modified along the Seine estuary. Furthermore, the sensitivity gain provided by the DNP allows the detection of ^{15}N NMR signal of DOM, in spite of the low content in nitrogen. These spectra reveal that the majority of nitrogen is in the amide form in these DOM samples and show an increased disorder around these amide groups near the mouth of the Seine.

Introduction

Dissolved organic matter (DOM) is one of the most mobile carbon pools at Earth's surface and is an important component of the global carbon cycle. Changes in the chemical or structural composition of DOM can drastically influence the aquatic ecosystem[1]. For example, DOM is a major source of energy and nutrients for bacteria in sea water. In this context, estuaries play a pivotal role in the transfer of DOM from the continents to the oceans. However, the transformations of DOM in estuaries are not yet well understood. [2-4]

The characterization of DOM is challenging owing to its structural complexity and heterogeneity. [5] It has been shown that solid-state nuclear magnetic resonance (ssNMR) spectroscopy can provide unique information on the atomic-level structure of DOM as well as the spatial and temporal changes in DOM composition. [6-8] Most ssNMR studies of DOM rely on the observation of ^{13}C nuclei, since ^{13}C ssNMR spectra of these samples exhibit good resolution and can be acquired within a day. Nevertheless, it has been shown that ^{15}N ssNMR of DOM can allow the identification of several nitrogen-containing functional groups, including amine, amide, and heterocyclic moieties, such as pyrrole and indole groups[9, 10]. However, ^{15}N isotope suffers from a low natural abundance (0.37%) and a low gyromagnetic ratio ($\gamma(^{15}\text{N})/\gamma(^1\text{H}) \approx 10.1\%$). Furthermore, atomic N/C ratios commonly range between 10^{-1} and 10^{-2} in DOM[11]. Consequently, conventional ssNMR detection of ^{15}N nuclei lacks sensitivity and requires acquisition times of several days, which often preclude the use of this technique.

Dynamic nuclear polarization (DNP) under magic-angle spinning (MAS), which is based on the microwave-driven transfer of polarization from unpaired electrons to the nuclear spins, can enhance the sensitivity of ssNMR[12, 13]. We have recently shown that DNP improves the sensitivity for the detection of ^{13}C nuclei in DOM by a factor of 4 with respect to conventional ssNMR, i.e. an acceleration of 16 in acquisition times. [14] The sensitivity gain provided by DNP has been leveraged to detect NMR signals of ^{15}N nuclei in organic, hybrid and inorganic materials[15-20]. However, to the best of our knowledge, it has never been applied to record ^{15}N NMR spectra of DOM.

DNP-enhanced NMR is applied herein to probe the local ^{13}C and ^{15}N environments as well as the functional groups in DOM of the Seine estuary.

Experimental session

Samples

Four water samples (100 liters each) were collected in April 2015 at mid-depth along the three parts of the Seine estuary: upstream (Caudebec), in the maximum of turbidity zone (Tancarville and Fatouville) and downstream (Honfleur) (Fig. 1). [4] All samples were filtered at 0.7 μm using glass fiber filters, concentrated to a few liters and desalted using reverse osmosis and electrodialysis before being concentrated further and freeze-dried, as described in ref. [4]

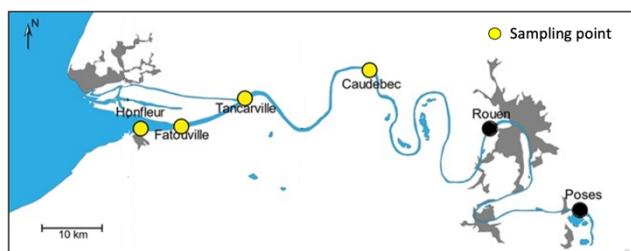


Figure 1. Map of the Seine estuary in France with the location of the sampling sites (yellow dots).

Scanning electron microscopy

The SEM images were recorded on an Itachi S-3400N equipped with a tungsten filament operating at an acceleration voltage of 15.0 kV. The powder is sprinkled on a double-sided carbon tape and then a carbon deposit is made to avoid charge effects.

DNP-enhanced NMR

For DNP-NMR experiments, the DOM samples were impregnated in the air with 10 mM AMUPol solution in $[\text{}^2\text{H}_8]\text{-glycerol}/[\text{}^2\text{H}_2]\text{O}$ (60/40 v/v) or $[\text{}^2\text{H}_6]\text{-dimethylsulfoxide (DMSO)}/[\text{}^2\text{H}_2]\text{O}/\text{H}_2\text{O}$ (78/14/8 w/w/w). The mass of DOM and the volume of AMUPol solution are given in Table S1. The investigated samples were packed into a 3.2 mm sapphire rotor closed with zirconia caps.

DNP experiments were performed at 9.4 T using a Bruker BioSpin Avance III DNP NMR spectrometer equipped with a triple-resonance $^1\text{H}/\text{X}/\text{Y}$ 3.2 mm low-temperature MAS probe and a gyrotron generating a continuous 263 GHz microwave irradiation[21]. The microwave irradiation was transmitted through a corrugated waveguide to the NMR MAS probe, and its power delivered to the sample was ca. 6 W. For all experiments, the B_0 field was 9.4 T, which corresponds to ^1H , ^{13}C and ^{15}N Larmor frequencies of 400.0, 100.6 and 40.6 MHz, respectively. The samples were spun at a MAS frequency of $\nu_R = 8$ kHz. The DNP-NMR spectra were acquired at a temperature of ca. 110 K, which was stabilized using a Bruker BioSpin MAS cooling system.

The $^1\text{H} \rightarrow ^{13}\text{C}$ CPMAS spectra were recorded with and without microwave (μw). The DNP enhancements, $\epsilon_{\text{on/off}}$, of the NMR signals were measured as the ratios between the NMR signals intensities with and without microwave irradiations under the same experimental conditions. The ^1H $\pi/2$ pulse duration was equal to 3 μs , while the cross-polarization (CP) contact times were equal to 50 μs in Fig. 5 and 3.5 ms in Figs. 2 and 4. During the CP transfer, the radio-frequency (RF) nutation frequency on the ^{13}C channel was constant and equal to 62.5 kHz, whereas the ^1H RF nutation frequency was linearly ramped from 50 to 100 kHz. SPINAL-64 decoupling with a ^1H nutation frequency equal to 47 kHz was applied during the acquisition of the ^{13}C free induction decay (FID).[22] The $^1\text{H} \rightarrow ^{13}\text{C}$ CPMAS spectra result from averaging 512 transients with a recovery delay of 0.73 s, i.e. an experimental time of 7 min. The ^{13}C isotropic chemical shifts were referenced to

tetramethylsilane (TMS) using the O=C group at 176.5 ppm of 30% ^{15}N - ^{13}C labeled glycine sample in 20 mM TOTAPol in glycerol- d_8 /D $_2$ O/H $_2$ O (6/3/1, w/w/w) as a secondary reference.

The $^1\text{H} \rightarrow ^{15}\text{N}$ CPMAS spectra were recorded with microwave irradiation. For $^1\text{H} \rightarrow ^{15}\text{N}$ CPMAS transfer, the ^1H $\pi/2$ pulse duration and the contact time were 2.75 μs and 3 ms, respectively. During the CP transfer, the ^1H RF nutation frequency was linearly ramped from 50 to 100 kHz, whereas the ^{15}N RF field amplitude was constant and equal to 45 kHz. SPINAL-64 ^1H decoupling was applied during the acquisition of ^{15}N spectra with an RF amplitude of 60 kHz. The $^1\text{H} \rightarrow ^{15}\text{N}$ CPMAS spectra were acquired with a recycle delay of 0.73 s. The number of transients and experimental times for the various samples are given in Table S2. The ^{15}N isotropic chemical shifts were referenced to nitromethane using the resonance of ^{15}N -labeled γ -glycine (−347.6 ppm) as a secondary reference[23, 24]. The $^1\text{H} \rightarrow ^{15}\text{N}$ CPMAS spectra were simulated using the DMfit software[25].

Results and discussion

The conventional $^1\text{H} \rightarrow ^{13}\text{C}$ CPMAS spectra of DOM shown in Fig. S1 were recorded in experimental times ranging from 15 to 23 h. They show resonances typical of riverine DOM[8, 26-28], including a broad peak ranging from 0 to 60 ppm assigned to aliphatic carbon sites, an intense signal at 72 ppm with a shoulder at 107 ppm produced by O-alkyl and anomeric groups in carbohydrates, a broad resonance with maximum at 130 ppm corresponding to aromatic and phenolic C sites and a carboxyl/amide signal at 175 ppm. The relative intensities of the various functional groups only weakly vary between the different samples. Hence, the local environments of ^{13}C nuclei remain mostly unchanged along the Seine estuary.

Nevertheless, a limitation of these conventional $^1\text{H} \rightarrow ^{13}\text{C}$ CPMAS experiments is the duration of these experiments. MAS DNP was used to circumvent this issue. For that purpose, these samples were impregnated with solutions of AMUPol[29] nitroxide biradicals, which is currently one of the most efficient polarizing agent for DNP-NMR experiments at 9.4 T and 100 K. We tested two different 10 mM AMUPol solutions, using either $[\text{}^2\text{H}_8]$ -glycerol/ $[\text{}^2\text{H}_2]\text{O}$ (60/40 v/v) or $[\text{}^2\text{H}_6]$ -dimethylsulfoxide (DMSO)/ $[\text{}^2\text{H}_2]\text{O}$ /H $_2\text{O}$ (78/14/8 w/w/w) mixtures as solvents. These solvents form glasses at 100 K and are partially or fully deuterated. Using a glass-forming deuterated solvent has been shown to be an efficient approach to improve the DNP enhancement[13, 30].

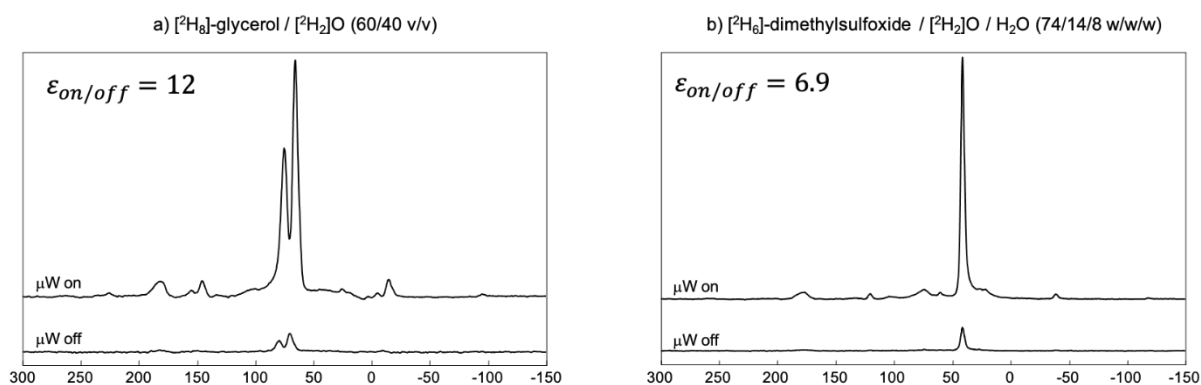


Figure 2. $^1\text{H} \rightarrow ^{13}\text{C}$ CPMAS NMR spectra with and without μW irradiation of DOM from Caudebec impregnated with 10 mM AMUPol solutions in (a) $[\text{}^2\text{H}_8]$ -glycerol/ $[\text{}^2\text{H}_2]\text{O}$ and (b) $[\text{}^2\text{H}_6]$ -DMSO/ $[\text{}^2\text{H}_2]\text{O}$ /H $_2\text{O}$ mixtures at 9.4 T and 110 K with a MAS frequency $\nu_r = 8$ kHz, CP contact time of 3.5 ms

Table 1. ^{13}C DNP-enhancement for the four samples impregnated with either AMUPol solutions in glycerol/water or DMSO/water. Enhancements $\epsilon_{\text{on/off}}$ are calculated by a comparison of the signal intensity with and without the microwaves on the peak resonating at 180 ppm on the ^{13}C spectrum for a spinning speed of 8 kHz.

	Caudebec	Tancarville	Fatouville	Honfleur
$\epsilon_{\text{on/off}}$ ^{13}C (180 ppm) glycerol/water	12	4	4.5	4
$\epsilon_{\text{on/off}}$ ^{13}C (180 ppm) DMSO/water	6.9	N/A	1.8	3.4

Fig. 2 shows the $^1\text{H} \rightarrow ^{13}\text{C}$ CPMAS spectra of DOM from Caudebec impregnated with AMUPol solutions. DNP enhances the ^{13}C NMR signals of DOM and the solvent by transferring the polarization of unpaired electrons to protons. This DNP-enhanced ^1H polarization is subsequently transferred to ^{13}C nuclei by CPMAS. For instance, DNP enhances the ^{13}C signal at 180 ppm assigned to carboxyl and amide sites by a factor $\epsilon_{\text{on/off}} = 12$, i.e., an acceleration factor of 144 in acquisition time, for the DOM from Caudebec impregnated with AMUPol solution in glycerol/water (Fig. 2a). In practice, the DNP-enhanced $^1\text{H} \rightarrow ^{13}\text{C}$ CPMAS spectrum of DOM from Caudebec was acquired in 7 min, instead of 22 h for the conventional spectrum of Fig. S1a. Table 1 reports DNP enhancements of this signal for the other samples. These enhancements are lower than 6 for the DOM collected downstream of Caudebec for both samples impregnated with glycerol/water and DMSO/water mixtures. The DNP enhancement has been reported to decrease when the size of the particles increases[31]. The size of the DOM material resulting from the isolation and desalting by reverse osmosis/electrodialysis was investigated by SEM and we noted an increase in the particle size downward the estuary (Fig. 3), which may be responsible for the decrease in DNP efficiency. These $\epsilon_{\text{on/off}}$ values measured for Seine DOM samples are comparable to those previously measured for DOM of Siberian rivers (5 to 10) with DMSO/water solutions of AMUPOL[14]. Furthermore, both the $\epsilon_{\text{on/off}}$ factors and the mass sensitivity, defined as the signal-to-noise ratio per square root of unit of time for a constant mass of sample, were higher for glycerol/water than DMSO/water. For instance, for DNP-enhanced $^1\text{H} \rightarrow ^{13}\text{C}$ CPMAS experiments on DOM from Caudebec, the mass sensitivity was equal to 90 and $40 \text{ s}^{-1/2} \cdot \text{g}^{-1}$ when the sample was impregnated with glycerol/water and DMSO/water, respectively. Due to a very low amount of DOM from Tancarville (Table S1), this sample could only be impregnated with one AMUPol solution. The glycerol/water solution was chosen as it yielded higher sensitivity for DOM from Caudebec.

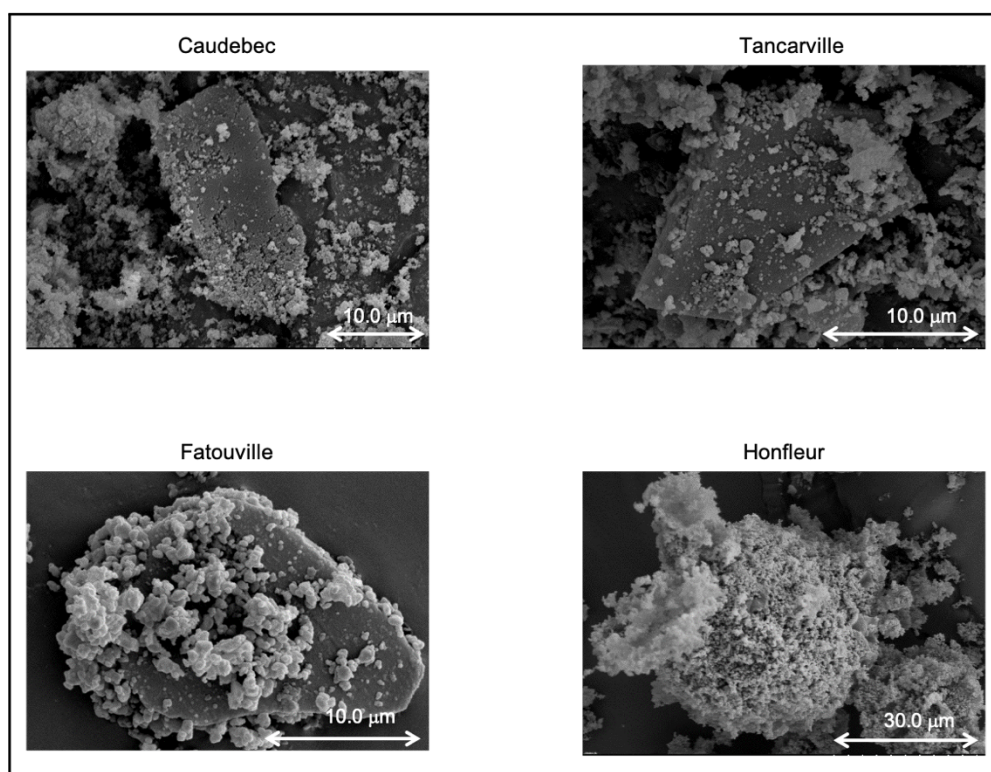


Figure 3. SEM images of DOM from Caudebec, Tancarville, Fatouville and Honfleur. The magnification are x3000 for Caudebec, x5000 for Tancarville and Fatouville x5000 and x1500 for Honfleur.

Table 2. Average size and standard deviation for each compound calculated by averaging the sizes of 20 particles

	Average size (μm^2)	Standard deviation (μm^2)
Caudebec	230	10
Tancarville	150	6
Fatouville	425	14
Honfleur	2,500	27

Fig. 4 shows the DNP-enhanced $^1\text{H} \rightarrow ^{13}\text{C}$ CPMAS spectra with a contact time of 3.5 ms of DOM impregnated with AMUPol solutions. Despite the use of deuterated solvents, limiting the ^1H - ^{13}C polarization transfer, the spectra are dominated by the ^{13}C NMR signals of the solvent, overlapping the DOM signals. However, the regions of the DOM spectrum masked by the solvent signal depend on the solvent. For the samples impregnated with glycerol/water mixture, the ^{13}C signals at 75 and 62 ppm assigned to the 2-C and 1,2-C sites of glycerol overlap with those of O-alkyl signals of DOM, whereas for the samples impregnated with DMSO/water mixture, the ^{13}C signal of DMSO at 41 ppm is superimposed on that of the aliphatic groups. Nevertheless, the ^{13}C signals of carboxyl/amide, anomeric and aliphatic functionalities can be observed for both solvents, whereas the ^{13}C signal of the O-alkyl group is clearly resolved for the samples impregnated with DMSO/water mixture. As shown in Fig. 5, the ^{13}C signal of deuterated glycerol and DMSO can be reduced by using short contact time in CPMAS in order to selectively transfer the DNP-enhanced ^1H polarization to the protonated ^{13}C sites of the DOM, but not to the deuterated ^{13}C nuclei of the solvent[32, 33]. Nevertheless, this approach prevents the observation of the carboxyl and amide sites, which are also not protonated.

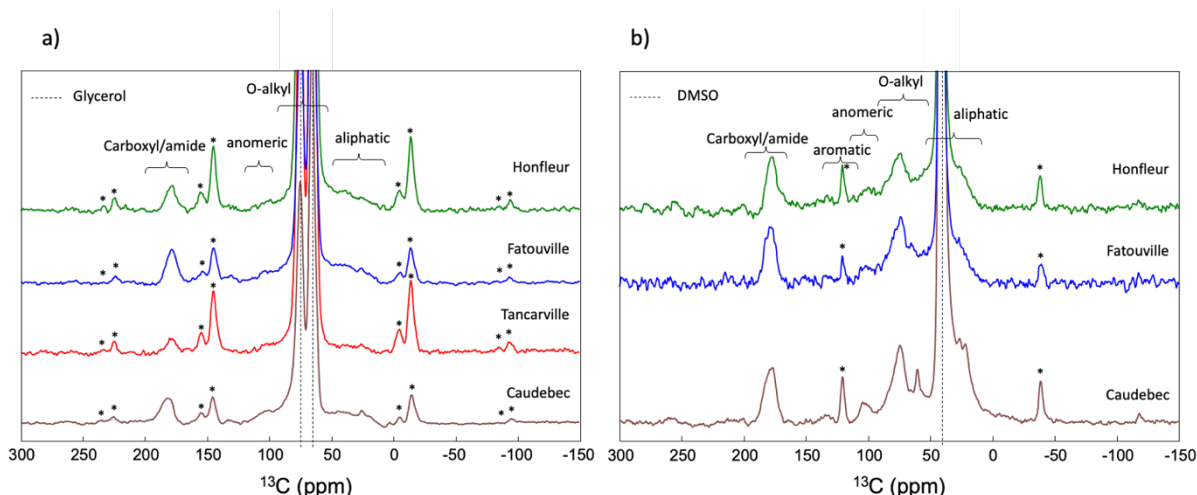


Figure 4. 1D $^1\text{H} \rightarrow ^{13}\text{C}$ CPMAS DNP NMR spectra of DOM from Caudebec (brown), Tancarville (red), Fatouville (blue) and Honfleur (green) impregnated with 10 mM AMUPol solutions in (a) $[\text{D}_8]\text{-glycerol}/[\text{D}_2]\text{O}$ and (b) $[\text{D}_6]\text{-DMSO}/[\text{D}_2]\text{O}/\text{H}_2\text{O}$ mixtures at 9.4 T and 110 K with a MAS frequency $\nu_r = 8$ kHz, CP contact time of 3.5 ms and microwave irradiation. Asterisks denote the spinning sidebands. It should be noticed that a spinning speed of 10 kHz was also tested [not shown] in order to check that the spinning sidebands of the carbonyl group do not overlap with the aliphatic resonances.

The relative intensities of the different ^{13}C sites in Figs. 4 and 5 are similar for the different DOM samples. This observation is consistent with the conventional $^1\text{H} \rightarrow ^{13}\text{C}$ CPMAS spectra of Fig. S1 and confirms that the local environment of ^{13}C nuclei in DOM is mostly unchanged along the Seine estuary. This agreement between conventional and DNP-enhanced NMR spectra indicates notably that the impregnation with AMUPol solution does not alter the atomic-level structure of DOM. Although DNP-enhanced and conventional $^1\text{H} \rightarrow ^{13}\text{C}$ CPMAS spectra provide similar information, DNP accelerates the acquisition of the ^{13}C signals by two orders of magnitude with respect to conventional NMR.

After having optimized and validated the use of DNP for the observation of ^{13}C nuclei in estuarine DOM, we investigated how the sensitivity gain provided by DNP can facilitate the detection of ^{15}N NMR signals of these samples. The NMR detection of this isotope is challenging owing to (i) the low natural abundance of ^{15}N isotope (0.37%), (ii) to the low nitrogen content in the DOM (< 1%) and (iii) the low amount of sample (Table S2). To the best of our knowledge, DNP has never been applied to accelerate the acquisition of ^{15}N NMR spectra of DOM. In DNP-enhanced $^1\text{H} \rightarrow ^{15}\text{N}$ CPMAS spectra, the cross-polarization transfers the DNP-enhanced ^1H polarization to the nearby ^{15}N nuclei and hence, the DNP enhancements for $^1\text{H} \rightarrow ^{13}\text{C}$ and $^1\text{H} \rightarrow ^{15}\text{N}$ CPMAS experiments are expected

to be similar. Given the higher DNP enhancement and

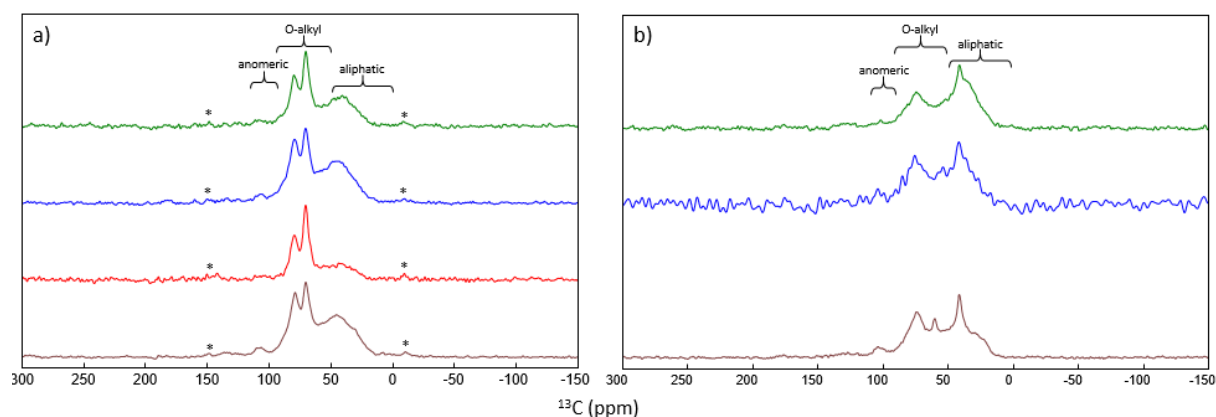


Figure 5. 1D DNP-enhanced $^1\text{H} \rightarrow ^{13}\text{C}$ CPMAS NMR spectra of DOM from Caudebec (brown), Tancarville (red), Fatouville (blue) and Honfleur (green) impregnated with 10 mM AMUPol solutions in (a) $[\text{^2H}_6]\text{-glycerol}/[\text{^2H}_2]\text{O}$ and (b) $[\text{^2H}_6]\text{-DMSO}/[\text{^2H}_2]\text{O}/\text{H}_2\text{O}$ mixtures at 9.4 T and 110 K with a MAS frequency $\nu_r = 8$ kHz, CP contact time of 50 μs and microwave irradiation. Asterisks denote the spinning sidebands.

mass sensitivity for the glycerol/water mixture in the case of $^1\text{H} \rightarrow ^{13}\text{C}$ CPMAS spectra, $^1\text{H} \rightarrow ^{15}\text{N}$ CPMAS spectra were only acquired for DOM samples impregnated with glycerol/water mixture (see Fig. 6). Sensitivity enhancement provided by DNP allows the detection of ^{15}N signals of these isotopically unmodified DOM within a reasonable experimental time (≤ 64 h), in spite of the low N/C atomic ratios (Tables 3 and S2, the organic and nitrogen contents of investigated DOM samples were determined by elemental analysis). Assuming similar sensitivity enhancements due to DNP for $^1\text{H} \rightarrow ^{13}\text{C}$ and $^1\text{H} \rightarrow ^{15}\text{N}$ CPMAS experiments, the latter would require more than a year without DNP. To the best of our knowledge, these spectra are the first DNP-enhanced ^{15}N NMR spectra of DOM reported so far. The $^1\text{H} \rightarrow ^{15}\text{N}$ CPMAS spectra are dominated by a peak resonating at ^{15}N isotropic chemical shift $\delta_{\text{iso}} \approx -259$ ppm assigned to amide group[24]. As seen in Table 4 and in Fig. 6, the broadening of this peak for the DOM from Fatouville and Honfleur indicates a larger distribution of local environments for the amide groups near the mouth of the Seine, where a decrease of the riverine vs. marine fraction of DOM occurs ⁴. Furthermore, the ^{15}N spectrum of DOM from Caudebec exhibits a broad shoulder centred at -216 ppm, which could subsume the contributions of substituted pyrrole and pyrrole functional groups[24]. Nevertheless, as the signal-to-noise ratio of this broad shoulder is low, its absence for the DOM sampled at other sites may result from the lower DNP enhancements. It is noted that even though amide functional groups are dominant in soil, sediment or dissolved organic matter, pyrrole groups can also be observed. In riverine DOM, the relative abundance of pyrrolic vs. amide groups was shown to be dependent on the river[24]. The relative abundance of pyrrole groups in DOM was suggested to be dependent on diagenetic (i.e. degradation) processes. The DNP-enhanced $^1\text{H} \rightarrow ^{15}\text{N}$ CPMAS spectra provide information on the presence of amide group and their local environment, which cannot be obtained by $^1\text{H} \rightarrow ^{13}\text{C}$ CPMAS spectra since the ^{13}C signals of carboxyl and amide groups overlap.

Table 3. N/C ratio for the four samples determined by elemental analysis^[4].

	Caudebec	Tancarville	Fatouville	Honfleur
N/C ratio	0.0923	0.0927	0.0931	0.0814

Table 4. ^{15}N isotropic chemical shift and FWHM (full width at half maximum) used to simulate the 1D $^1\text{H} \rightarrow ^{15}\text{N}$ CPMAS spectra of Fig. 5 (see the simulated spectra shown in Fig. 6).

	Caudebec	Tancarville	Fatouville	Honfleur
--	----------	-------------	------------	----------

δ_{iso} (ppm)	-216/-257	-261	-259	-257
FWHM (Hz)	2043/631	600	973	1100

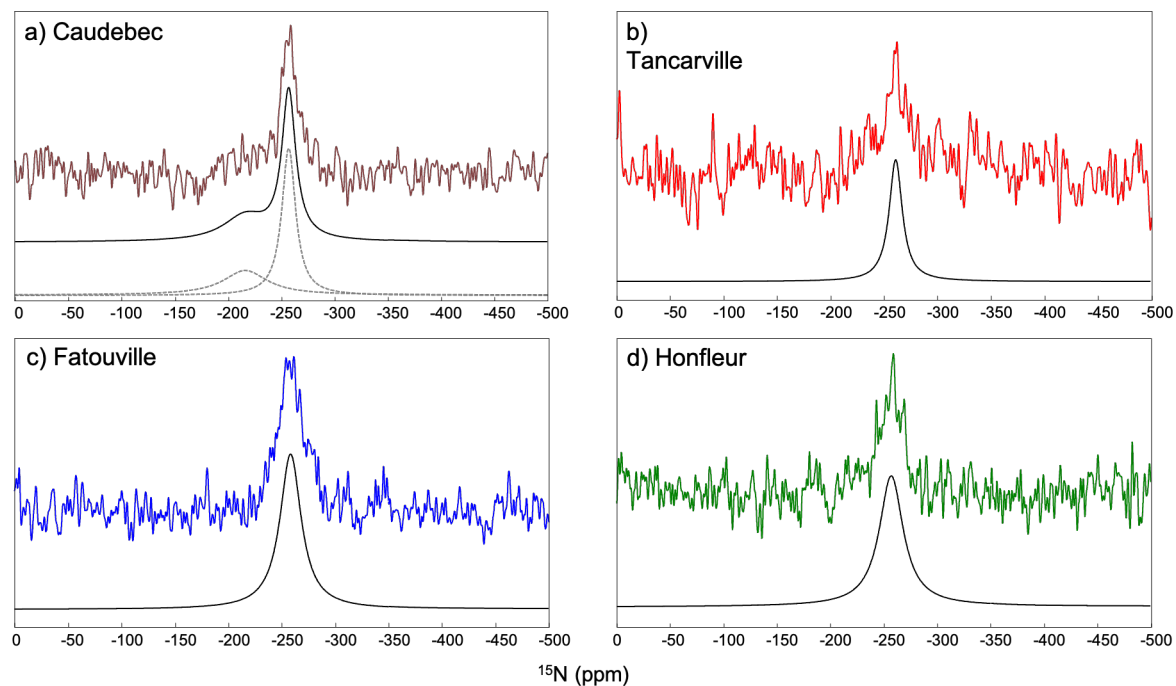


Figure 6. Experimental (blue) and simulated (red) DNP-enhanced $^1\text{H} \rightarrow ^{15}\text{N}$ CPMAS spectra of DOM from (a) Caudebec, (b) Tancarville, (c) Fatouville and (d) Honfleur impregnated with 10 mM AMUPol solution in $[\text{^2H}_2]\text{-glycerol}/[\text{^2H}_2]\text{O}$ mixture and with microwave irradiation. The spectra b, c and d were simulated with one component, whereas the spectrum a was simulated with one component. The NMR parameters of the simulated spectra are reported in Table 4. The full lines correspond to the DMFit simulation of the spectrum, while the dashed lines for the Caudebec spectrum represent the two components.

Conclusion

We applied DNP-enhanced ^{13}C and ^{15}N NMR spectroscopy to probe the functional groups in DOM collected along the three parts of the Seine estuary (the upstream zone, the maximum of turbidity zone and the downstream zone). DNP experiments were optimized and validated on $^1\text{H} \rightarrow ^{13}\text{C}$ CPMAS experiments. These DNP-enhanced ^{13}C NMR spectra indicate in agreement with conventional ^{13}C NMR spectra that the nature and the proportion of the different functional groups in DOM are unmodified in the different zones of the Seine estuary. Furthermore, we demonstrated for the first time the possibility using DNP under MAS to detect ^{15}N NMR signals of DOM samples, which contain low fraction of nitrogen atoms and are not amenable to ^{15}N isotopic enrichment. These NMR spectra show that most of nitrogen atoms in DOM are in the amide form. In addition, these NMR data indicate a broader distribution in the local environment of nitrogen atoms in DOM collected near the mouth of the Seine. The structural insights provided by DNP-enhanced ^{15}N NMR cannot be retrieved from the ^{13}C NMR spectra because of the overlap between ^{13}C carboxyl and amide NMR signals.

Acknowledgments

The Chevreul Institute (FR 2638), Ministère de l'Enseignement Supérieur, de la Recherche et de l'Innovation, Hauts-de-France Region, and FEDER are acknowledged for supporting and funding partially this work. Financial support from the contract Isite ULNE : MOFFIN-OPE-2019-43-5400 is gratefully acknowledged. We thank the GIP Seine-Aval through the funding of the MOSAIC project (2014-2017) during which the Seine estuary samples were collected. Alexandre Thibault, Edith Parlanti and Mahaut Sourzac are thanked for the collection and preparation of the DOM samples. V.K. acknowledges financial support by the AvH society.

Keywords

^{13}C , ^{15}N , DNP, DOM, Seine estuary

References

- [1] J. J. Middelburg, P. M. J. Herman *Mar. Chem.* **2007**, *106*, 127-147.
- [2] H. A. N. Abdulla, E. C. Minor, R. F. Dias, P. G. Hatcher *Geochim. Cosmochim. Acta.* **2013**, *118*, 231-246.
- [3] H. A. N. Abdulla, E. C. Minor, R. F. Dias, P. G. Hatcher *Geochim. Cosmochim. Acta.* **2010**, *74*, 3815-3838.
- [4] A. Thibault, S. Derenne, E. Parlanti, C. Anquetil, M. Sourzac, H. Budzinski, L. Fuster, A. Laverman, C. Roose-Amsaleg, E. Viollier, A. Huguet *Mari. Chem.* **2019**, *212*, 108-119.
- [5] J. E. Bauer, T. S. Bianchi *Treatise on Estuarine and Coastal Science, Vol 5: Biogeochemistry.* **2011**, 7-67.
- [6] H. Knicker *Org. Geochem.* **2011**, *42*, 867-890.
- [7] A. J. Simpson, D. J. McNally, M. J. Simpson *Prog. Nucl. Magn. Reson. Spectrosc.* **2011**, *58*, 97-175.
- [8] J. D. Mao, X. Y. Cao, D. C. Olk, W. Y. Chu, K. Schmidt-Rohr *Progr. Nucl. Magn. Reson. Spectrosc.* **2017**, *100*, 17-51.
- [9] M. McCarthy, T. Pratum, J. Hedges, R. Benner *Nature.* **1997**, *390*, 150-154.
- [10] L. I. Aluwihare, D. J. Repeta, S. Pantoja, C. G. Johnson *Science.* **2005**, *308*, 1007-1010.
- [11] K. A. Thorn, L. G. Cox *Org. Geochem.* **2009**, *40*, 484-499.
- [12] D. A. Hall, D. C. Maus, G. J. Gerfen, S. J. Inati, L. R. Becerra, F. W. Dahlquist, R. G. Griffin *Science.* **1997**, *276*, 930-932.
- [13] A. G. M. Rankin, J. Trebosc, F. Pourpoint, J. P. Amoureux, O. Lafon *Solid State Nucl. Magn. Reson.* **2019**, *101*, 116-143.
- [14] F. Pourpoint, J. Templier, C. Anquetil, H. Vezin, J. Trébosc, X. Trivelli, F. Chabaux, O. S. Pokrovsky, A. S. Prokushkin, J. P. Amoureux, O. Lafon, S. Derenne *Chem. Geol.* **2017**, *452*, 1-8.

- [15] A. J. Rossini, A. Zagdoun, M. Lelli, J. Canivet, S. Aguado, O. Ouari, P. Tordo, M. Rosay, W. E. Maas, C. Coperet, D. Farrusseng, L. Emsley, A. Lesage *Angew. Chem.-Int. Ed.* **2012**, *51*, 123-127.
- [16] A. J. Rossini, C. M. Widdifield, A. Zagdoun, M. Lelli, M. Schwarzwaelder, C. Coperet, A. Lesage, L. Emsley *J. Am. Chem. Soc.* **2014**, *136*, 2324-2334.
- [17] T. Gutmann, J. Q. Liu, N. Rothermel, Y. P. Xu, E. Jaumann, M. Werner, H. Breitzke, S. T. Sigurdsson, G. Buntkowsky *Chem. Eur. J.* **2015**, *21*, 3798-3805.
- [18] A. S. L. Thankamony, C. Lion, F. Pourpoint, B. Singh, A. J. P. Linde, D. Carnevale, G. Bodenhausen, H. Vezin, O. Lafon, V. Polshettiwar *Angew. Chem.-Int. Ed.* **2015**, *54*, 2190-2193.
- [19] S. Gratz, M. de Olivera, T. Gutmann, L. Borchardt *Phys. Chem. Chem. Phys.* **2020**, *22*, 23307-23314.
- [20] F. Blanc, S. Y. Chong, T. O. McDonald, D. J. Adams, S. Pawsey, M. A. Caporini, A. I. Cooper *J. Am. Chem. Soc.* **2013**, *135*, 15290-15293.
- [21] M. Rosay, L. Tometich, S. Pawsey, R. Bader, R. Schauwecker, M. Blank, P. M. Borchard, S. R. Cauffman, K. L. Felch, R. T. Weber, R. J. Temkin, R. G. Griffin, W. E. Maas *Phys. Chem. Chem. Phys.* **2010**, *12*, 5850-5860.
- [22] B. M. Fung, A. K. Khitrin, K. Ermolaev *J. Magn. Reson.* **2000**, *142*, 97-101.
- [23] P. Bertani, J. Raya, B. Bechinger *Solid State Nucl. Magn. Reson.* **2014**, *61-62*, 15-18.
- [24] J. Templier, F. Miserque, N. Barre, F. Mercier, J. P. Croue, S. Derenne *J. Anal. Appl. Pyrol.* **2012**, *97*, 62-72.
- [25] D. Massiot, F. Fayon, M. Capron, I. King, S. Le Calve, B. Alonso, J. O. Durand, B. Bujoli, Z. H. Gan, G. Hoatson *Magn. Reson. Chem.* **2002**, *40*, 70-76.
- [26] E. Kaiser, A. J. Simpson, K. J. Dria, B. Sulzberger, P. G. Hatcher *Environ. Sci. Technol.* **2003**, *37*, 2929-2935.
- [27] J. Templier, S. Derenne, J. P. Croue, C. Largeau *Org. Geochem.* **2005**, *36*, 1418-1442.
- [28] P. Conte, C. Abbate, A. Baglieri, M. Negre, C. De Pasquale, G. Alonzo, M. Gennari *Org. Geochem.* **2011**, *42*, 972-977.
- [29] C. Sauvée, M. Rosay, G. Casano, F. Aussenac, R. T. Weber, O. Ouari, P. Tordo *Angew. Chem.-Int. Ed.* **2013**, *52*, 10858-10861.
- [30] M. M. Rosay, **2001**, Sensitivity-enhanced Nuclear Magnetic Resonance of biological solids, Thesis, Massachusetts Institute of Technology. <http://dspace.mit.edu/handle/1721.1/119613>
- [31] A. C. Pinon, J. Schlagnitweit, P. Berruyer, A. J. Rossini, M. Lelli, E. Socie, M. X. Tang, T. Pham, A. Lesage, S. Schantz, L. Emsley *J. Phys. Chem. C.* **2017**, *121*, 15993-16005.
- [32] D. Lee, S. R. Chaudhari, G. De Paepe *J. Magn. Reson.* **2017**, *278*, 60-66.
- [33] J. R. Yarava, S. R. Chaudhari, A. J. Rossini, A. Lesage, L. Emsley *J. Magn. Reson.* **2017**, *277*, 149-153.